FEBS Letters 425 (1998) 448–452 FEBS 20047

Elucidation of the cause for reduced activity of abnormal human plasmin containing an Ala^{55}-Thr mutation: importance of highly conserved Ala^{55} in serine proteases

Mayuko Takeda-Shitaka*, Hideaki Umeyama

School of Pharmaceutical Sciences, Kitasato University, 5-9-1 Shirokane, Minato-ku, Tokyo 108-8641, Japan

Received 23 February 1998

Abstract In serine proteases, Ala^{55} is highly conserved and located just behind the catalytic triad. That the activity of human plasmin is reduced by the A55T substitution indicates the importance of Ala^{55} in catalysis. In the present study, the 3-D model of A55T human plasmin shows that an unusual hydrogen bond between Thr^{55} Oγ1 and His^{57} Nε2 alters His^{57} into an inactive conformation in which His^{57} cannot accept a proton from Ser^{195} as a catalytic base. Our results demonstrate that Ala^{55} contributes heavily to the active conformation of His^{57} and ensures the proton transfer from Ser^{195} to His^{57}.

Key words: Serine protease; Plasmin; Homology modeling; Molecular dynamics simulation

1. Introduction

Throughout the large family of trypsin-like serine proteases, the catalytic triad of His^{57}, Asp^{102} and Ser^{195} (Fig. 1; chymotrypsinogen numbering is used in the present paper) is completely conserved. The catalytic roles of these residues have been well established by experimental [1–4] and theoretical [5,6] evidence. Serine proteases catalyze the hydrolysis of amides and esters by nucleophilic attacks on the carbonyl carbon of the scissile bond by the hydroxyl group of Ser^{195}. His^{57} acts as a catalytic base which enhances the nucleophilicity of Ser^{195} and assists proton transfer from the serine hydroxyl to the substrate leaving group. Asp^{102} Oδ atoms (Oδ1 and Oδ2) stabilize the side-chain conformation of His^{57} that is required for catalysis by accepting hydrogen bonds from His^{57} Nδ1.

In addition to the catalytic triad, neighboring residues, such as Cys^{42}, Gly^{43}, Ala^{55}, Cys^{58}, Tyr/Phe/Trp^{94}, Gly^{196}, Gly^{197} and Ser^{214}, are almost completely conserved in both the primary and tertiary structures [7,8]. These residues together with the catalytic triad stabilize one another by intramolecular interactions conserved in serine proteases, which maintain the active conformation of the catalytic triad (Fig. 1). Among the conserved neighboring residues, Ala^{55} seems to be very important for catalysis, because X-ray structures show that Ala^{55} Cβ is located just behind the catalytic His^{57} and Asp^{102}.- Interestingly, there are many reports that reduced activity of human plasmin (HUPL) in patients with venous thrombosis and with retinochoroidal vascular disorders results from replacing Ala^{55} with Thr in the serine protease domain [9–14]. Previous experimental studies of A55T HUPL demonstrated that the patients possess normal levels of plasminogen antigen, and that its Michaelis constant is very similar to normal ones. In spite of these normal properties, A55T HUPL has low activity on the synthetic substrates [15,16]. These experimental results indicate that the cause of the reduced activity of A55T HUPL is localized in the catalytic site, whereas the overall structure of A55T HUPL is normal. Therefore, we investigated the structural features of the catalytic sites of normal and A55T HUPLs to reveal the role of the residue at position 55.

In the present paper, since the X-ray structures of normal and A55T HUPLs have yet to be solved, we constructed 3-D structures by homology modeling method. The catalytic sites of the models were evaluated using molecular dynamics (MD) simulations. Our results indicate that there are clear structural differences between the catalytic sites of normal and A55T HUPLs. The reduced activity of A55T HUPL probably results from the inability of His^{57} to act as the catalytic base.

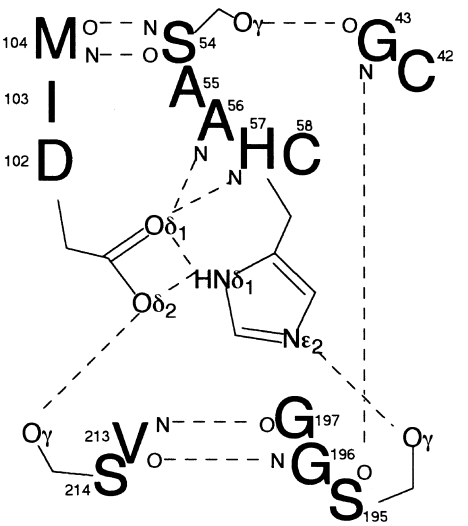

Fig. 1. Schematic representation of the hydrogen bonding network in the catalytic site of BOTR. In order to act as the catalytic base, His^{57} must conform to the following conditions: (i) monoprotonated His^{57} at optimum pH must be protonated at Nδ1 not Nε2 and (ii) His^{57} must be stabilized in the conformation in which Nε2 can accept a proton from Ser^{195} Oγ.

*Corresponding author. Fax: (81) (3) 3446-9553.
E-mail: shitakam@platinum.pharm.kitasato-u.ac.jp

Abbreviations: BOTR, bovine trypsin; HUPL, serine protease domain of human plasmin; MD simulation, molecular dynamics simulation; loop 5–6, loop between 5 and 6 β-strands in the N-terminal domain of serine protease

PII S0014-5793(98)00280-4

```
          16          26          36          46          56
HUPL   VVGGCVAHPHSWPWQVSLRTRFGMHFCGGTLISPEWVLTAA
BOTR   IVGGYTCGANTVPYQVSLNS--GYHFCGGSLINSQWVVSAA
                                                *
                      66          76          86
HUPL   HCLEKSPRPSSYKVILGAHQEVNLEPHVQEIEVSRLFLEPT
BOTR   HCY---KS--GIQVRLGEDNINVVEGNEQFISASKSIVHPS
       *
         96         106         116         126
HUPL   ------RKDIALLKLSSPAVITDKVIPACLPSPNYVVADRT
BOTR   YNSNTLNNDIMLIKLKSAASLNSRVASISLPT--SCASAGT
              *
        136         146         156         166
HUPL   ECFITGWGETQG--TFGAGLLKEAQLPVIENKVCNRYEFLN
BOTR   QCLISGWGNTKSSGTSYPDVLKCLKAPILSDSSCKS--AYP

         176         186         196         206
HUPL   GRVQSTELCAGHLAGGTDSCQGDSGGPLVCFEKDKYILQGV
BOTR   GQITSNMFCAGYLEGGKDSCQGDSGGPVVCSGK----LQGI
                                  *
           216         226         236
HUPL   TSWGLGCARPNKPGVYVRVSRFVTWIEGVMRNN
BOTR   VSWGSGCAQKNKPGVYTKVCNYVSWIKQTIASN
```

Fig. 2. Sequence alignment of HUPL and BOTR. Chymotrypsinogen numbering is indicated above the sequences. Residues marked with asterisks are catalytic triad and Ala[55]. Loop 5–6 is indicated by bold letters.

2. Materials and methods

2.1. Construction of the models

The 3-D structure of HUPL was constructed with the CHIMERA modeling system [17] based on the sequence of the serine protease domain of HUPL (residues 562–791, plasminogen numbering) [18]. The main chain was constructed by connecting the fragments of reference X-ray structures obtained from the Brookhaven Protein Data Bank (PDB) [19]: residues 16–18 (bovine trypsin; PDB code 4PTP), 19–41 (bovine chymotrypsin; 5CHA), 42–54 (4PTP), 55–64 (human u-PA; 1LMW), 65–67 (4PTP), 68–80 (human neutrophil elastase; 1HNE), 81–118 (4PTP), 119–138 (5CHA), 139–156 (4PTP), 157–180 (1LMW), 181–198 (4PTP), 199–210 (5CHA) and 211–245 (4PTP). Two loop searches in the PDB were performed at residues 92–101 and 145–150. The final structure derived from CHIMERA was refined by energy minimization with an AMBER united-atom force field [20] using the program APRICOT [21]. The program PROCHECK [22] was used to evaluate the stereochemical quality of the model. The A55T HUPL model was constructed based on the HUPL model by replacing Ala[55] with Thr, and was energy minimized using APRICOT.

2.2. Molecular dynamics simulation in the catalytic region

A cap of TIP3P water molecules [23] was placed 22 Å from His[57] Cε1 of the models. First the water molecules were energy minimized and then the whole system was energy minimized. All residues which lie 15 Å or more from His[57] Cε1 were fixed, while the residues within 15 Å and the water molecules were allowed to move during the course of MD simulation. The residues that construct the active site were all allowed to move. The whole system was thermalized from 0 to 300 K for 10 ps, and a 190 ps simulation was performed. The system was kept at 300 K during the productive simulation by applying a temperature coupling $\tau = 0.1$ ps. All calculations were carried out using APRICOT with AMBER united-atom force field, a non-bonded cutoff of 12 Å and a constant dielectric of 1. The SHAKE algorithm was applied to all bonds involving hydrogen atoms. A time step of 0.002 ps was used. Data were collected every 0.5 ps.

3. Results and discussion

3.1. HUPL and A55T HUPL models

First, in order to evaluate the accuracy of the model derived from CHIMERA, we constructed a model of bovine trypsin (BOTR) whose X-ray structure had been solved. The root mean square deviations for superposition between the main chain atoms in the model and in the corresponding X-ray structure are 0.90 Å (all residues) and 0.50 Å (residues lying within 15 Å of His[57] Cε1). The model was very similar to the X-ray structure, especially in the catalytic site region.

HUPL showed high sequence identities to the reference proteins, among which the sequence identity to BOTR was the highest (41.3%; Fig. 2). The HUPL model is shown in Fig. 3. The X-ray structure of BOTR is also shown in Fig. 3 for comparison. The orientation of the catalytic triad and the hydrogen bonding pattern in the catalytic site are conserved in the HUPL model. No unfavorable contacts between

Table 1
Hydrogen bonds in the catalytic sites[a] of HUPL and A55T HUPL models

Hydrogen bond partners	HUPL model		A55T HUPL model									
	Distance (Å)[b]	Time (%)[c]	Distance (Å)					Time (%)				
			0° [d]	30°	60°	180°	−60°	0°	30°	60°	180°	−60°
A56 N–D102 Oδ1[e]	2.89	43.7	2.83	2.87	2.77	2.85	2.80	45.1	86.7	34.2	70.9	44.7
H57 N–D102 Oδ1[e]	2.83	49.2	2.88	2.84	2.85	2.85	2.87	51.8	95.7	37.0	80.4	36.7
A56 N–D102 Oδ2[e]	2.90	46.5	2.88	2.96	2.87	2.84	3.15	46.1	2.2	58.0	20.3	0.7
H57 N–D102 Oδ2[e]	2.83	49.5	2.87	3.00	2.84	2.91	3.01	51.8	4.2	63.7	22.5	1.5
H57 Nδ1–D102 Oδ1[e]	2.93	93.5	2.89	2.96	2.90	2.93	2.94	68.1	72.5	90.5	79.4	34.2
H57 Nδ1–D102 Oδ2[e]	2.95	95.0	2.96	2.91	2.96	2.89	2.95	69.4	77.5	88.5	79.6	34.2
D102 Oδ1[e]–S214 Oγ	3.04	7.2	–	–	3.03	3.00	3.23	0	0	2.5	2.7	0.2
D102 Oδ2[e]–S214 Oγ	2.76	26.0	2.76	2.75	2.73	2.75	2.78	21.3	33.7	30.2	28.5	14.5
H57 Nε2–S195 Oγ	3.10	0.7	3.18	3.18	3.07	3.14	3.15	1.7	4.0	1.2	5.7	1.0
T54 N–A104 O	2.86	99.5	2.89	2.91	2.93	2.89	2.92	98.7	99.7	99.0	100	99.5
T54 O–A104 N	2.85	99.7	2.85	2.86	2.88	2.85	2.88	98.9	99.5	99.2	99.4	99.7
G43 O–T54 Oγl	2.87	99.0	2.91	2.91	2.93	2.90	2.91	94.7	96.5	94.2	96.2	97.7
G43 N–S195 O	2.92	98.2	2.88	2.88	2.91	2.91	2.88	98.4	98.7	97.2	98.7	99.2
G196 N–T213 O	2.85	97.7	2.86	2.89	2.89	2.84	2.83	99.7	97.7	99.2	99.7	99.7
G197 O–T213 N	3.00	90.5	2.98	3.08	3.00	2.99	2.99	94.2	86.5	88.5	92.7	95.2

[a]The hydrogen bonds in the catalytic site are schematically shown in Fig. 1, in which positions 54, 104 and 213 are Thr, Ala and Thr, respectively, in HUPL.
[b]The distances are average distances of snapshots where the interactions are characterized as hydrogen bonds (2.4–3.4 Å) during MD simulations.
[c]Times (%) are percentages of snapshots where the interactions are characterized as hydrogen bonds during MD simulations.
[d]The starting χ1 values of Thr[55] in MD simulations of A55T HUPL.
[e]When there are rotations of the χ2 angle of Asp[102], Asp[102] Oδ1 and Oδ2 alternate in accepting the hydrogen bonds from Ala[56] N, His[57] N, His[57] Nδ1 and Ser[214] Oγ.

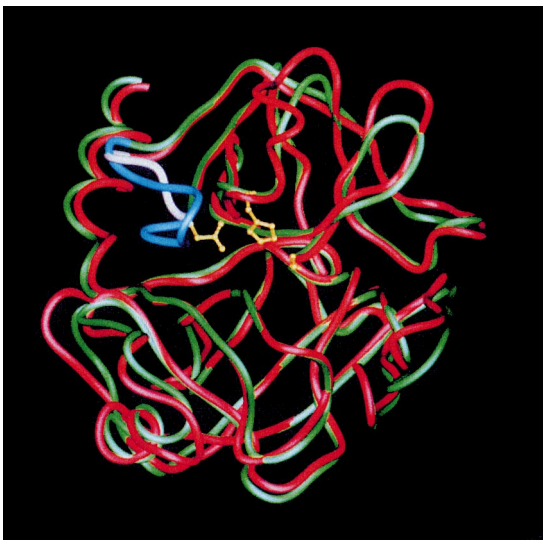

Fig. 3. Tube diagram of the superposition of the main chains of the HUPL model (red) and the X-ray structure of BOTR (green; PDB code 4PTP). The side chains of the catalytic triad of the HUPL model are shown in yellow. Loop 5–6 of BOTR is shown in blue and that of HUPL is shown in white.

the atoms and no unnatural chiral centers are observed. In the Ramachandran plot of the main-chain ϕ-φ angles, all of the non-glycine residues are in the most favored or allowed regions. The main-chain ω angles are all trans-planar. In general serine proteases, Asp[102] is fully shielded from the solvent by seven highly conserved residues [24], Ala[55], Ala[56], His[57], Cys[58], Tyr[94], Leu[99] and Ser[214] in BOTR for example, but is partially buried in the HUPL model. Two of the seven residues (position 94 and 99) are included in the loop between 5 and 6 β-strands in the N-terminal domain (loop 5–6), but HUPL lacks these two residues because loop 5–6 is small

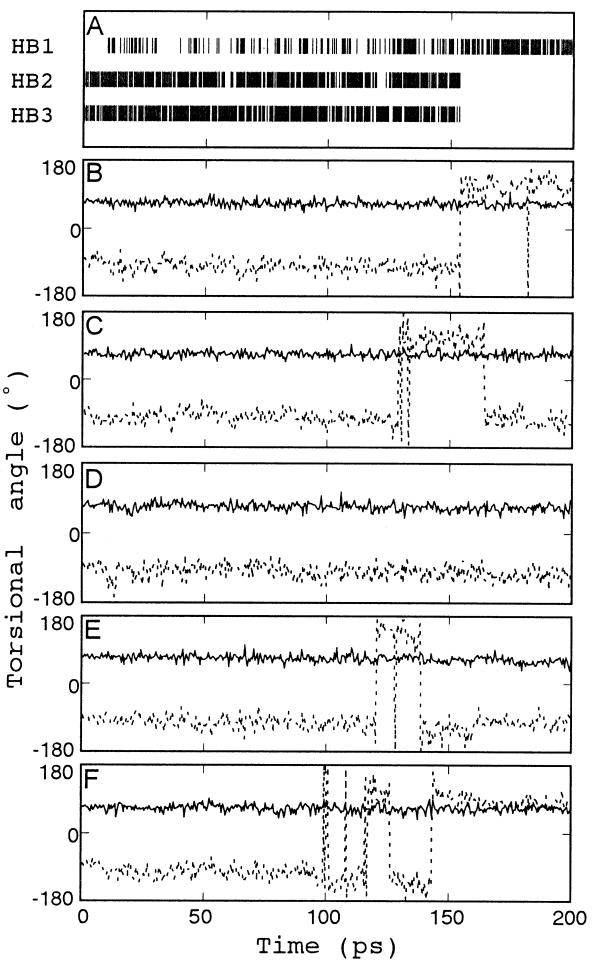

←

Fig. 4. Dynamic properties of the catalytic site of A55T HUPL in MD simulations. The starting χ1 value of Thr[55] were 0° (A and B), 30° (C), 60° (D), 180° (E) and −60° (F). A: Small bars denote the formation of the hydrogen bonds between Thr[55] Oγ1 and His[57] Nε2 (HB1), between His[57] Nδ1 and Asp[102] Oδ1 (HB2) and between His[57] Nδ1 and Asp[102] Oδ2 (HB3). B–F: The χ1 (solid lines) and χ2 (dottd lines) values of His[57].

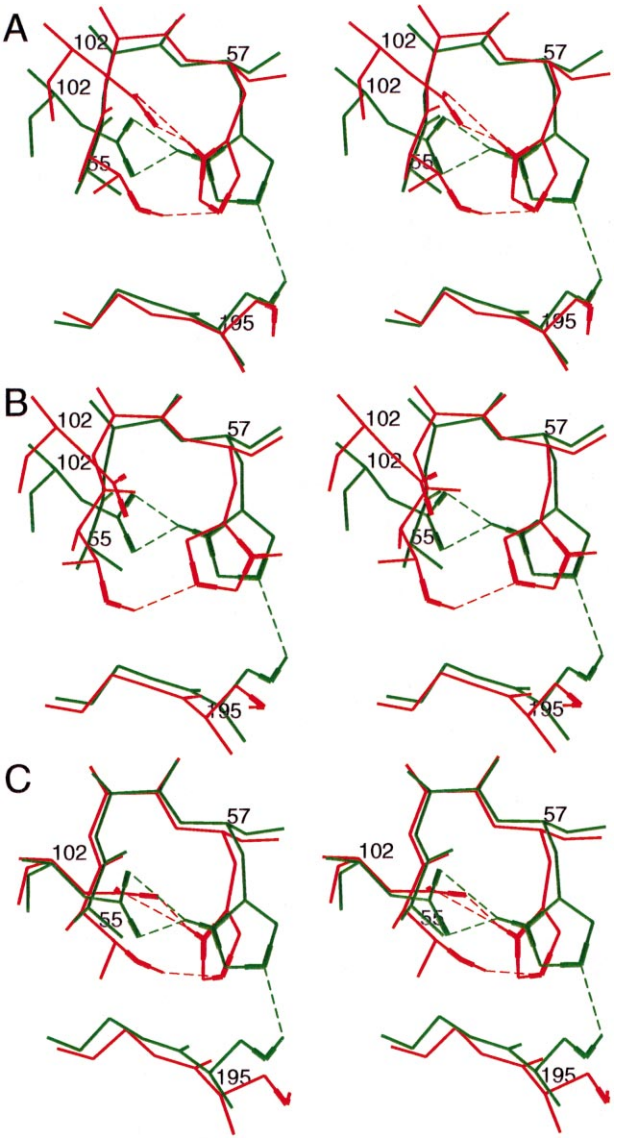

Fig. 5. Stereo views of the catalytic triad and Ala/Thr[55]. Thr[55] Oγ1, His[57] Nδ1, His[57] Nε2, Asp[102] Oδ atoms and Ser[195] Oγ are drawn with thicker lines. The hydrogen bonds are drawn with dotted lines. The hydrogen atoms (Thr[55] HOγ1, His[57] HNδ1 and Ser[195] HOγ) are shown. Green: Active conformation of HUPL (A and B) and BOTR (C). Red: Conformations A and B of A55T HUPL (A and B, respectively) and conformation A of A55T BOTR (C).

(Figs. 2 and 3). Therefore Asp[102] in the HUPL model is not fully buried. Experimental results demonstrate that plasmin has considerable room in the loop 5–6 region [25,26].

In the A55T HUPL model refined by energy minimization, the A55T substitution appears to have no bad effect on the catalytic site in spite of its reduced activity. The hydrogen bonding pattern in the catalytic site is similar to the normal one, and the catalytic triad is in the active conformation. However, further evaluation of the model is required as shown in the next section, because while refinement by energy minimization is able to remove short contacts among atoms, it is not able to correct any serious errors in the model.

3.2. Evaluation of the models by molecular dynamics simulations

We performed MD simulations of the models to investigate whether the hydrogen bonding pattern in the catalytic site and the active conformation of the catalytic residues are maintained or not. The dynamic properties of the hydrogen bonds in the catalytic site are presented in Table 1. In the simulation of the HUPL model, the orientation of the His[57] side chain was stably maintained. Due to 180° rotations of the side-chain torsional angle χ2 of Asp[102] (Cα-Cβ-Cγ-Oδ1), Asp[102] Oδ1 and Oδ2 alternated in accepting the hydrogen bonds from Ala[56] N, His[57] N and Ser[214] Oγ. All but two of the hydrogen bonds in the catalytic site were stably maintained during the simulation. The exceptions were the hydrogen bond between His[57] Nε2 and Ser[195] Oγ, and the hydrogen bond between Asp[102] Oδ1/Oδ2 and Ser[214] Oγ. The former was lost. This hydrogen bond is thought to be formed after substrate is bound [27]. The latter was effective 7.2% (between Asp[102] Oδ1 and Ser[214] Oγ) and 26.0% (between Asp[102] Oδ2 and Ser[214] Oγ) of the simulation time. This hydrogen bond may not always be necessary for catalysis, because S214A rat anionic trypsin is more active than native ones [28]. The result of our simulation was in good agreement with those of whole unconstrained MD simulations of the X-ray structures of BOTR [29] and porcine pancreatic elastase [30], suggesting that the catalytic sites of normal serine proteases show similar dynamic properties and that the catalytic region of the HUPL model is accurate enough.

For A55T HUPL, we performed five MD simulations to investigate the preferred side-chain conformation of Thr[55]; the starting χ1 values of Thr[55] (N-Cα-Cβ-Oγ1) were 0°, 30°, 60°, 180° and −60°, respectively. Independent of the starting conformation, Thr[55] was only in the gauche$^-$ conformation (mean χ1 value = 28.8°). The backbone-dependent rotamer library [31] also shows that the suitable conformation for Thr[55] is gauche$^-$. The most remarkable feature of A55T HUPL is the formation of an unusual hydrogen bond between Thr[55] Oγ1 and His[57] Nε2 (HB1 in Fig. 4A). It is never formed in normal serine proteases, because the side chain of Ala[55] includes no hetero atoms that can be hydrogen bond donor to His[57] Nε2. Although this unusual hydrogen bond was not found by energy minimization because Thr[55] Oγ1 and His[57] Nε2 were not close to each other at first, it was found in all five MD simulations. It was not stable at first but gradually became stable. The catalytic site of A55T HUPL had two conformations A and B. Fig. 4A,B shows the results of one of five simulations. As shown in Fig. 4A, the normal hydrogen bonds between His[57] Nδ1 and Asp[102] Oδ atoms were maintained together with the unusual hydrogen bond at first (conformation A; Fig. 5A). Next, the hydrogen bonds between His[57] Nδ1 and Asp[102] Oδ atoms were lost (HB2 and HB3 in Fig. 4A) and there was a rotation of the χ2 angle of His[57] (Fig. 4B), which produced another conformation B (Fig. 5B). The form of the unusual hydrogen bond in conformation B is different from that in conformation A. Also in the other three simulations, both conformations A and B were found due to the rotation of the χ2 angle of His[57] (Fig. 4C,E,F). In some simulations, conformation A is found again due to the second rotation of the χ2 angle of His[57] (Fig. 4C,E). Conformation B was not found in one of five simulations, in which the catalytic site is only in conformation A (Fig. 4D). A55T HUPL has a slightly higher isoelectric point (p*I*) than normal [15]. Our results indicate that the different p*I* value of A55T HUPL results from the conformational changes of the catalytic residues that probably accompany the changes of the charge distribution.

3.3. The cause of reduced activity of A55T HUPL

The unusual hydrogen bond between Thr[55] Oγ1 and His[57] Nε2 due to the A55T substitution alters His[57] into the unusual conformation. Fig. 5A,B shows conformations A and B of A55T HUPL, together with the corresponding active conformations of HUPL. To act as the catalytic base normally, His[57] Nε2 has to be able to accept a proton from Ser[195] Oγ as drawn in green in Fig. 5A,B (schematically shown in Fig. 1). In conformation A, however, it is difficult for His[57] to accept the proton from Ser[195], because His[57] Nε2 retreats from Ser[195] Oγ toward Thr[55] Oγ1 to accept the hydrogen bond from Thr[55] Oγ1 (drawn in red in Fig. 5A). Also in conformation B, His[57] is clearly unable to accept the serine hydroxyl proton because the His[57] conformation is quite different from normal one (drawn in red in Fig. 5B). This indicates that His[57] in A55T HUPL is unable to act as the catalytic base and enhance the nucleophilicity of Ser[195] effectively. The studies of D102N rat trypsin demonstrate that the inability of His[57] to act as the catalytic base reduces protease activity [1,2]. Also in the case of A55T HUPL, the reduced activity probably results from the inability of His[57] to act as the catalytic base, although the immediate cause of it is different from that of D102N trypsin.

In A55T HUPL, Asp[102] moved from the normal position as shown in Fig. 5A,B. Asp[102] in A55T HUPL is not stabilized by the surrounding residues because loop 5–6 is unusually small as described above, so that Asp[102] may be greatly influenced by the steric hindrance caused by the A55T substitution, and the hydrogen bonds between His[57] Nδ1 and Asp[102] Oδ atoms tend to become lost, which produces conformation B. We constructed the A55T BOTR model for comparison. In the case of A55T BOTR, Asp[102] itself and the hydrogen bonds between His[57] Nδ1 and Asp[102] Oδ atoms are stabilized by the neighboring residues. In the resulting model of A55T BOTR, Asp[102] and the hydrogen bonds between His[57] Nδ1 and Asp[102] Oδ atoms are not disordered by the A55T substitution as expected, and A55T BOTR is only in conformation A (Fig. 5C). Both A55T HUPL and A55T BOTR models show that conformation B is not found when Asp[102] and the hydrogen bonds between His[57] Nδ1 and Asp[102] Oδ atoms are stable. A55T HUPL is probably in conformation A over conformation B when substrate binds, because substrate may fill the space provided by the unusual small loop 5–6 of A55T HUPL and the environment of Asp[102] becomes similar to that of

A55T BOTR. This suggestion is reasonable because conformation A is seems to have slight activity, which agrees with the experimental data that A55T HUPL retains slight activity (k_{cat} is 10 times lower than normal [16]). The A55T BOTR model indicates that the activity of A55T mutants of serine proteases other than A55T HUPL is reduced.

The X-ray structures of normal serine proteases show that the region where the proton transfer from Ser^{195} to His^{57} occurs is completely conserved in both the primary and tertiary structures throughout this family. Moreover, this region is stabilized by the common hydrogen bonding network in this family. In this region, there are no hetero atom candidates for the hydrogen bond donor to His^{57} Nε2 except Ser^{195} Oγ, which probably ensures the proton transfer from Ser^{195} Oγ to His^{57} Nε2 after the substrate binds. These completely conserved structural features indicate that the steric requirement of the proton transfer is very strict, which means that the activity can be reduced by a slight change of this region. In the case of A55T mutants, the unusual hydrogen bond between His^{57} Nε2 and Thr^{55} Oγ1 disturbs the proton transfer from Ser^{195} to His^{57}, which reduces the protease activity.

4. Conclusions

In conclusion, the present study demonstrates that the residue at position 55 provides an important contribution to the active conformation of the catalytic residues. In the case of A55T HUPL, since His^{57} Nε2 unusually accepts the hydrogen bond from Thr^{55} Oγ1 and retreats from Ser^{195} Oγ, His^{57} is unable to accept the serine hydroxyl proton and enhance the nucleophilicity of Ser^{195} effectively. The reduced activity of A55T HUPL is probably caused by the inability of His^{57} to act as the catalytic base. On the other hand, in the case of normal serine proteases, Ala^{55} has no hetero atoms that can be hydrogen bond donor to His^{57} Nε2, and, therefore, His^{57} is in the active conformation and is able to accept a proton from Ser^{195} as the catalytic base after substrate is bound. The present study will shed new light on the essential environment for the catalysis of serine proteases.

Acknowledgements: We thank Dr. Shigetaka Yoneda for helpful discussions. This work was supported by a grant-in-aid for special project research from the Ministry of Education, Science, Sports and Culture in Japan.

References

[1] Sprang, S., Standing, T., Fletterick, R.J., Stroud, R.M., Finer-Moore, J., Xuong, N.H., Hamlin, R., Rutter, W.J. and Craik, C.S. (1987) Science 237, 905–909.
[2] Craik, C.S., Roczniak, S., Largman, C. and Rutter, W.J. (1987) Science 237, 909–913.
[3] Corey, D.R. and Craik, C.S. (1992) J. Am. Chem. Soc. 114, 1784–1790.
[4] Corey, D.R., McGrath, M.E., Vásquez, J.R., Fletterick, R.J. and Craik, C.S. (1992) J. Am. Chem. Soc. 114, 4905–4907.
[5] Umeyama, H., Hirono, S. and Nakagawa, S. (1984) Proc. Natl. Acad. Sci. USA 81, 6266–6270.
[6] Warshel, A., Naray-Szabo, G., Sussman, F. and Hwang, J.K. (1989) Biochemistry 28, 3629–3637.
[7] Rypniewski, W.R., Perrakis, A., Vorgias, C.E. and Wilson, K.S. (1994) Protein Eng. 7, 57–64.
[8] Lesk, A.M. and Fordham, W.D. (1996) J. Mol. Biol. 258, 501–537.
[9] Miyata, T., Iwanaga, S., Sakata, Y. and Aoki, N. (1982) Proc. Natl. Acad. Sci. USA 79, 6132–6136.
[10] Miyata, T., Iwanaga, S., Sakata, Y., Aoki, N., Takamatsu, J. and Kamiya, T. (1984) J. Biochem. 96, 277–287.
[11] Ichinose, A., Espling, E.S., Takamatsu, J., Saito, H., Shinmyozu, K., Maruyama, I., Petersen, T.E. and Davie, E.W. (1991) Proc. Natl. Acad. Sci. USA 88, 115–119.
[12] Li, L., Kikuchi, S., Arinami, T., Kobayashi, K., Tsuchiya, S. and Hamaguchi, H. (1994) Clin. Genet. 45, 285–287.
[13] Tsutsumi, S., Saito, T., Sakata, T., Miyata, T. and Ichinose, A. (1996) Thromb. Haemost. 76, 135–138.
[14] Murata, M., Ooe, A., Izumi, T., Nakagawa, M., Takahashi, S., Ishikawa, M., Mori, K. and Ichinose, A. (1997) Br. J. Haematol. 99, 301–303.
[15] Aoki, N., Moroi, M., Sakata, Y. and Yoshida, N. (1978) J. Clin. Invest. 61, 1186–1195.
[16] Sakata, Y. and Aoki, N. (1980) J. Biol. Chem. 255, 5442–5447.
[17] Yoneda, T., Komooka, H. and Umeyama, H. (1997) J. Protein Chem. 16, 597–605.
[18] Petersen, T.E., Martzen, M.R., Ichinose, A. and Davie, E.W. (1990) J. Biol. Chem. 265, 6104–6111.
[19] Bernstein, F.C., Koetzle, T.F., Williams, G.J.B., Meyer Jr., E.F., Brice, M.D., Rodgers, J.R., Kennard, O., Shimanouchi, T. and Tasumi, M. (1977) J. Mol. Biol. 112, 535–542.
[20] Weiner, S.J., Kollman, P.A., Case, D.A., Singh, U.C., Ghio, C., Alagona, G., Profeta Jr., S. and Weiner, P. (1984) J. Am. Chem. Soc. 106, 765–784.
[21] Yoneda, S. and Umeyama, H. (1992) J. Chem. Phys. 97, 6730–6736.
[22] Laskowski, R.A., McArthur, M.W., Moss, D.S. and Thornton, J.M. (1993) J. Appl. Crystallogr. 26, 283–291.
[23] Jorgensen, W.L., Chandrasekhar, J. and Madura, J.D. (1983) J. Chem. Phys. 79, 926–935.
[24] Blow, D.M., Birktoft, J.J. and Hartley, B.S. (1969) Nature 221, 337–340.
[25] Matsuzaki, T., Sasaki, C. and Umeyama, H. (1988) J. Biochem. 103, 537–543.
[26] Matsuzaki, T., Sasaki, C., Okumura, C. and Umeyama, H. (1989) J. Biochem. 105, 949–952.
[27] Perona, J.J. and Craik, C.S. (1995) Protein Sci. 4, 337–360.
[28] McGrath, M.E., Vásquez, J.R., Craik, C.S., Yang, A.S., Honig, B. and Fletterick, R.J. (1992) Biochemistry 31, 3059–3064.
[29] Heimstad, E.S., Hansen, L.K. and Smalås, A.O. (1995) Protein Eng. 8, 379–388.
[30] Geller, M., Carlson-Golab, G., Lesyng, B., Swanson, S.M. and Meyer Jr., E.F. (1990) Biopolymers 30, 781–796.
[31] Dunbrack Jr., R.L. and Karplus, M. (1993) J. Mol. Biol. 230, 543–574.